Equation of state for weakly coupled quantum plasmas

J. Vorberger,* M. Schlanges, and W. D. Kraeft
Institut für Physik, Ernst-Moritz-Arndt-Universität Greifswald, Domstrasse 10a, 17489 Greifswald, Germany
(Received 13 November 2003; published 29 April 2004)

We calculate thermodynamic properties for a dense hydrogen plasma and a quantum electron gas using thermodynamic Green's function techniques. Our perturbation approach is appropriate to give reliable results in the weak coupling regime. In particular, the contribution of the exchange term of the order e^4 is fully included for the nondegenerate case as well as for the dense highly degenerate quantum region. We compare our results for the equation of state with data obtained by different numerical simulations.

DOI: 10.1103/PhysRevE.69.046407 PACS number(s): 52.25.Kn, 52.27.Aj, 52.27.Gr

I. INTRODUCTION

An exact knowledge of thermodynamic properties, e.g., of hydrogen or deuterium, is of great importance not only for scientific reasons but also for technical applications. The models of the inner structure of stars or giant gas planets depend on the equation of state (EOS) data and so do model calculations concerning inertially confined fusion experiments. Shock experiments on hydrogen and deuterium [1–3] are usually evaluated by discussing hugoniots, for which the theoretical inputs are EOS data. The comparison of different hugoniots shows essential differences both between different experiments and between different theories including numerical simulations, and on the other hand also between theory and experiment [4–6]. For this reason it seems to be desirable to have reliable EOS data in limiting situations where the theoretical approximations are justified. We have then to demand that the numerical simulations coincide with analytical results. The region in between which is not accessible to theoretical treatment should then be covered by numerical simulations or at least by Padé formulas [7].

The aim of this paper is to investigate the thermodynamic properties of dense quantum plasmas using quantum statistical theory. In particular, the imaginary time Green's function technique is applied, which turned out to be a powerful method for describing physical properties of dense quantum plasmas in thermodynamic equilibrium [9,10].

First, the basic equations are presented and the scheme of approximation is given which is applied in the subsequent calculations. The numerical evaluation of the EOS is described in detail in Sec. III. The different contributions such as the Montroll-Ward and the e^4 exchange terms as well as the inversion procedure are discussed. Finally, we present results for thermodynamic quantities for the electron gas and the fully ionized hydrogen plasma. Pressure and internal energy are compared to wave-packet molecular-dynamics (WPMD) calculations and to data obtained by path-integral Monte Carlo (PIMC) simulations.

II. BASIC EQUATIONS AND APPROXIMATIONS

Considering the plasma in the grand canonical ensemble the EOS can be calculated using the charging formula [8–10]

$$(p-p_0)\Omega = -\int_0^1 \frac{d\lambda}{\lambda}\langle \lambda V\rangle. \tag{1}$$

Here $p-p_0$ is the excess part of the pressure, Ω the volume of the system, $\langle \lambda V\rangle$ the mean potential energy, and λ the interaction strength parameter. In second quantization the two-particle Green's function G_{ab} determines the mean potential energy[1]

$$\langle \lambda V\rangle = \frac{\lambda}{2}\sum_{a\sigma_a}\sum_{b\sigma_b}\int_0^{-i\beta} d1\,dr_2 V_{ab}(12) \times G_{ab}(121^{++}2^{+})|_{t_2=t_1^+}. \tag{2}$$

We used, e.g., $1=\mathbf{r}_1,t_1$. In the case of a plasma consisting of charged particles of species a and b the interaction potential is the Coulomb potential, i.e., $V_{ab}(\mathbf{r}_1-\mathbf{r}_2)=q_a q_b/|\mathbf{r}_1-\mathbf{r}_2|$. All statistical information is contained in G_{ab}. For Coulomb systems, it is convenient to account for collective effects by introduction of a screened potential V^s_{ab} defined by the screening equation

$$V^s_{ab}(12) = V_{ab}(12) + \sum_{cd}\int_0^{-i\beta} d\bar{1}d\bar{2}V^s_{ac}(1\bar{1})\Pi_{cd}(\overline{21},\overline{21})V_{db}(\bar{2}\bar{2}). \tag{3}$$

Now the polarization function Π_{ab} replaces the two-particle Green's function, while the screened potential appears instead of the Coulomb one:

$$\langle \lambda V\rangle = \frac{1}{2}\sum_{a\sigma_a}\sum_{b\sigma_b}\int d1\,dr_2\{\lambda V_{ab}(12)G_a(11^{++})G_b(22^{+}) + V^s_{ab}(12,\lambda)\Pi_{ab}(12,12)\}. \tag{4}$$

Here the Hartree term appears separately (the first term on the right-hand side) while it is still included in Eq. (2). Equation (4) is our starting point for further calculations. We do not discuss the general problem, which cannot be solved ex-

*Electronic address: jan.vorberger@physik.uni-greifswald.de

[1]We use Heaviside units, $\hbar=1$, $e^2=2$, $2m_e=1$, $a_B=1$.

 ©2004 The American Physical Society

actly. For the goal of this paper it is sufficient to give the first terms of a perturbation series for the polarization function; for further details see [9]:

$\Pi(12,1'2') \approx$ 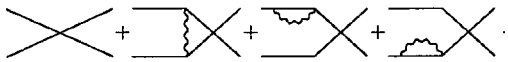 (5)

These terms have their origin in the screened ladder approximation of the polarization function. The wavy lines denote dynamically screened potentials determined by Eq. (3). From left to right we see the random phase approximation (RPA) contribution, the vertex term (first ladder diagram), and two first order self-energy contributions to the Green's functions of the RPA. If this series of terms is inserted into Eq. (4), we get the following contributions to the mean value of the potential energy. We want to establish a perturbation expansion in powers of e^2, i.e., in powers of the Coulomb potential. For this purpose, we express all screened potentials with the help of the screening equation (3) and take into account only terms with powers up to e^4 (two potential lines) [11]:

$\langle \lambda V \rangle \approx$ 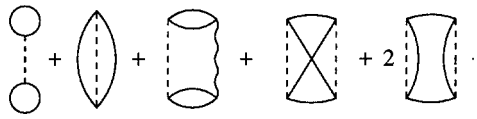 (6)

From left to right we see the Hartree, Hartree-Fock (HF), Montroll-Ward (MW), normal e^4 exchange, and anomalous e^4 exchange terms. The first gives the mean field contribution. This term vanishes in a quasineutral system. The second term (HF) is the exchange term of order e^2. The MW term is the first nonideality correction due to the Coulomb interaction. Here one screened potential must be retained in order to keep this term convergent. In the low density limit the MW contribution is the Debye-Hückel correction to the ideal gas result. The HF and MW terms arise from the RPA approximation of the polarization function Π_{ab}. The first ladder term of the polarization function (vertex) gives the fourth term in this series, the normal exchange term of order e^4. The last two identical graphs are a result of first order self-energy corrections to the RPA and are called anomalous e^4 exchange terms. This expansion will be denoted the e^4 expansion in the rest of the paper although the MW term contains infinite powers of e^2 in the screened potential to avoid Coulomb divergences. This series takes into account only weak interactions. Therefore it can be used to describe weakly coupled plasmas ($\Gamma \leqslant 1$, $\Gamma = \langle E_{pot} \rangle / \langle E_{kin} \rangle$). No approximations have been made concerning the degeneracy of the plasma. The Fermi statistics is fully included. So this expansion provides a good approximation for the low density and for the high density (nonrelativistic) plasma.

Using Eqs. (1) and (6) we get the pressure as a function of the chemical potential μ for a weakly coupled quantum plasma:

$$p(\{\beta\mu_c\}) = \sum_a \frac{\zeta_a}{\beta} I_{3/2}(\beta\mu_a) + \sum_a \zeta_a \xi_a \mathcal{I}_{HF}(\beta\mu_a) + p^{MW}(\{\beta\mu_c\}) + \sum_a p_a^{e^4 n}(\beta\mu_a) + \sum_a p_a^{e^4 a}(\beta\mu_a). \quad (7)$$

The arrangement of the terms is nearly the same as in Eq. (6). The ideal contribution is followed by the HF, the MW, and both of the e^4 exchange terms. Some abbreviations were used: $\zeta_a = (2\sigma_a + 1)/\Lambda_a^3$ and $\xi_a = e_a^2/\Lambda_a$. The sum runs over the species. $\Lambda_a^2 = 2\pi/(m_a k_B T)$ is the thermal wavelength, $\beta = 1/(k_B T)$ the inverse temperature, $I_{3/2}$ the Fermi integral of order 3/2, and $\mathcal{I}_{HF}$ the HF integral [12] $\mathcal{I}_{HF} = \int_{-\infty}^{\beta\mu_a} d\alpha I_{-1/2}^2(\alpha)$. The density is given by $n_a = \partial p / \partial \mu_a$,

$$n_a(\{\beta\mu_c\}) = \zeta_a I_{1/2}(\beta\mu_a) + \zeta_a \xi_a I_{-1/2}^2(\beta\mu_a) + \frac{\partial}{\partial \mu_a}[p^{MW}(\{\beta\mu_c\}) + p_a^{e^4 n}(\beta\mu_a) + p_a^{e^4 a}(\beta\mu_a)]. \quad (8)$$

Further explicit calculations require the numerical evaluation of the different contributions. Having pressure and density as a function of the chemical potential, one has to eliminate the latter to get the usual EOS, i.e., the pressure as a function of the density. This is done in the next sections.

III. NUMERICAL TREATMENT

A. Special contributions

The calculation of the main input quantities for both pressure and internal energy requires some numerical effort. In this section we want to analyze the different contributions and give some results, especially for the e^4 exchange terms.

In full generality the MW term is given in terms of the (longitudinal) dielectric function $\varepsilon(p,\omega)$,

$$p^{MW}(\{\beta\mu_c\}) = -\frac{1}{4\pi^3} \int_0^\infty p^2 dp \mathcal{P} \int_0^\infty d\omega \coth\left(\frac{\beta\omega}{2}\right) \times \left[\arctan \frac{\mathrm{Im}\,\varepsilon(p,\omega)}{\mathrm{Re}\,\varepsilon(p,\omega)} - \mathrm{Im}\,\varepsilon(p,\omega)\right]. \quad (9)$$

In this term it is sufficient to take the dielectric function in the random phase approximation. For the treatment of degenerate quantum plasmas it is necessary to retain full dynamics in the screening of the Coulomb potential and in the dielectric function. In general, the calculation of the MW term means computing a three-dimensional integral (two plus one in the real part of the dielectric function). Figure 1 shows the behavior of the MW pressure from the low density/nondegenerate to the high density/degenerate region for fully ionized hydrogen. We want to remark that, in contrast to the exchange terms of order e^4, this term is not simply the sum

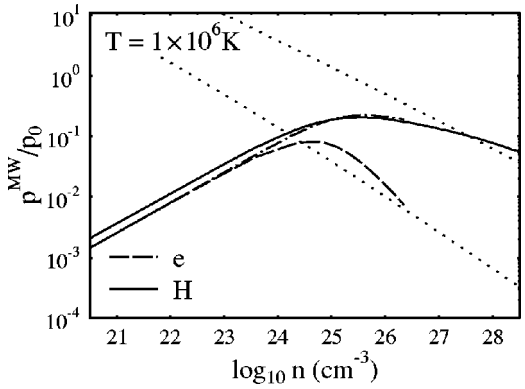

FIG. 1. Ratio of MW pressure and ideal pressure for hydrogen (solid) and an electron gas (dashed) as functions of the electron density. The $T=0$ results (dotted) are additionally shown (upper, hydrogen; lower, electron gas). The dash-dotted line gives the Debye-Hückel low density result for the electron gas.

of electron and proton contributions. Due to electron-proton correlations it cannot be split into a sum over the species.

The normal exchange term of order e^4 can be written in momentum-frequency space as

$$p^{e^4n}(\{\beta\mu_c\})=\Omega\sum_a m_a\int \frac{d\mathbf{p}d\mathbf{q}_1d\mathbf{q}_2}{(2\pi)^9} \times\frac{V_{aa}(\mathbf{p})V_{aa}(\mathbf{p}+\mathbf{q}_1+\mathbf{q}_2)}{q_1^2+q_2^2-(\mathbf{p}+\mathbf{q}_1)^2-(\mathbf{p}+\mathbf{q}_2)^2} \times\{f_a(q_1)f_a(q_2)[1-f_a(\mathbf{q}_1+\mathbf{p})] \times[1-f_a(\mathbf{q}_2+\mathbf{p})]-f_a(\mathbf{q}_1+\mathbf{p})f_a(\mathbf{q}_2+\mathbf{p}) \times[1-f_a(q_1)][1-f_a(q_2)]\}. \tag{10}$$

Here V_{aa} is the bare Coulomb potential and f_a are Fermi functions. After some manipulations there remain only six integrations. The integrations can be done using Monte Carlo integration. Both in the low density and in the high density region, the exactly known limiting results for this integral [9,13] are reproduced with high accuracy. In Fig. 2 this term is shown for a temperature of $T=10^6$ K as a function of the electron degeneracy parameter $n\Lambda_e^3$. In this case, the excess pressure contribution according to Eq. (1) can be calculated as $p^{e^4n}=-(1/2)\langle V\rangle^{e^4n}$ from the mean exchange energy. For low degeneracy it is dominated by the electrons, whereas the protons determine the behavior of this contribution for higher values of the electron degeneracy parameter.

For purposes discussed below we still consider the anomalous e^4 term and analyze especially its limiting behavior. The term reads

$$p^{e^4a}(\{\beta\mu_c\})=-2\Omega\beta\sum_a \int \frac{d\mathbf{k}d\mathbf{p}d\mathbf{q}}{(2\pi)^9}V_{aa}(\mathbf{q}-\mathbf{k}) \times V_{aa}(\mathbf{q}-\mathbf{p})f_a(\mathbf{k})f_a(\mathbf{p})f_a(\mathbf{q})[1-f_a(\mathbf{q})]. \tag{11}$$

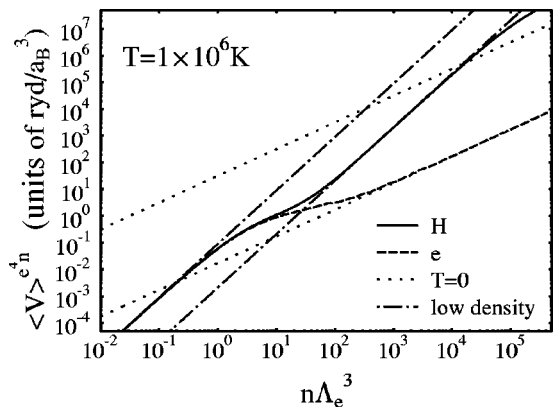

FIG. 2. Normal e^4 exchange energy for hydrogen (solid) and an electron gas (dashed) as function of the electron degeneracy $n\Lambda_e^3$. Additionally, low density (dash-dotted: upper curve, electrons; lower curve, protons) and $T=0$ limiting results (dotted: upper curve, protons; lower curve, electrons) are shown.

The evaluation is simple and can easily be extended to regions where exact limiting results are known. Figure 3 shows the behavior of this term, which is very similar to that of the normal e^4 exchange term.

With the knowledge of all of the terms in Eq. (7), calculation of thermodynamic quantities is now possible.

B. Inversion and thermodynamic quantities

Now the contributions to the EOS given by Eq. (7) are explicitly known. Therefore all thermodynamic quantities are determined on this level of approximation. Because of Eqs. (7) and (8) we have an EOS in the grand canonical ensemble. In any case, we have to satisfy the condition of quasineutrality in the two-component plasma, i.e., for a given chemical potential μ_a of species a Eq. (8) defines the corresponding chemical potential μ_b due to $\Sigma_c e_c n_c=0$. Although there is such an equation of state as a function of the fugacity z_a ($z_a=e^{\beta\mu_a}$), it is also of great importance to get the explicit

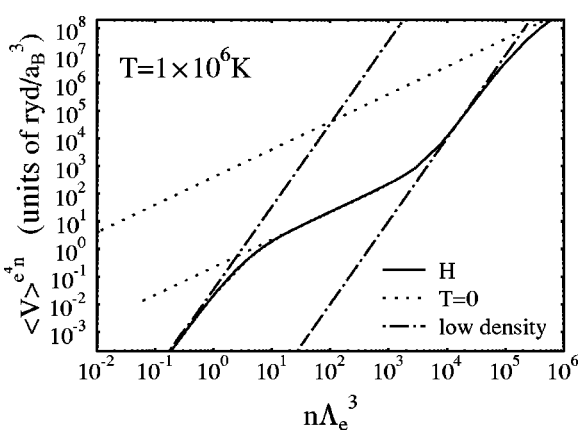

FIG. 3. Anomalous e^4 exchange energy for hydrogen (solid) as function of the electron degeneracy parameter $n\Lambda_e^3$. Additionally, low density (dash-dotted: upper curve, electrons, lower curve, protons) and $T=0$ limiting results (dotted: upper curve, protons; lower curve, electrons) are shown.

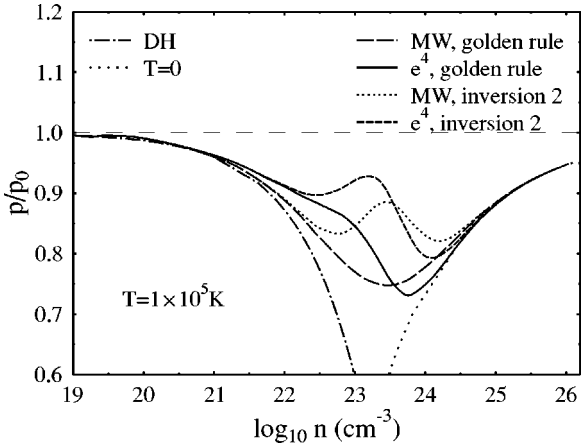

FIG. 4. Pressure with respect to the ideal part for an electron gas as function of the density. Different approximations and different types of inversion for the EOS are shown. The solid curve (e^4, golden rule) is given by Eq. (12). MW means that the normal e^4 exchange term is omitted. DH denotes the low density Debye-Hückel correction to the ideal gas. The $T=0$ curve is the limiting result of Gell-Mann and others [13,16].

dependence on the density $p=p(n)$. This procedure of the elimination of the fugacity from the pressure $p=p(\{z_c\})$ through $n_a=z_a(\partial/\partial z_a)\beta p(\{z_c\})$ is called inversion. This means having the thermodynamic quantities in the grand canonical ensemble first and then going to the canonical ensemble. Equations (7) and (8) are no fugacity expansions in the usual sense. They contain all powers of the fugacity as a consequence of the quantum nature of the treated systems, which is fully included in our approach.

To solve Eq. (8) analytically for the fugacity is impossible. Furthermore, to have such an expression would not necessarily result in a more exact equation of state than using approximate equations for the fugacity. This is due to the approximation in the starting equations. Because of our limitation of taking into account only powers up to e^4 the final expression should also contain only terms up to the same order.

The inversion procedure is done in detail as follows [14]. We split the chemical potential into an ideal and different interaction parts each containing zero, one ($\sim e^2$), two ($\sim e^4$), or more interactions $\mu=\mu^0+\mu^{(1)}+\mu^{(2)}+\cdots$. In our case it is appropriate to suggest that $\mu^{(i)}\ll\mu^0\ \forall i\epsilon\mathcal{N}$. Then we can do a Taylor expansion of Eq. (8) around μ^0. In this way we get expressions for all of the interaction parts of the chemical potential as functions of the free chemical potential if we demand that the density is given by $n_a=\zeta_a I_{1/2}(\beta\mu_a^0)$. According to our starting approximation all terms of higher order in the interaction than e^4 are dropped. Doing the same Taylor expansion in Eq. (7) and inserting the results for the interaction contributions of the chemical potential as obtained in the previous step, we get the pressure in the canonical ensemble as a function of the free chemical potential μ^0 and thus of the density. This procedure we call inversion 2, and the curves obtained with this inversion can be seen in Fig. 4.

The pressure due to inversion 2 is correct in the interaction order but suffers from a different shortcoming. In the low density nondegenerate case this expansion becomes a real density expansion, but is inconsistent in the order of the density. So we have to neglect the anomalous e^4 exchange term, because it is of order n^3. At $T=0$, the same term is compensated by some contributions arising from our inversion procedure [15]. Therefore we completely omit the anomalous exchange term and the compensation terms. This procedure can be summarized under the so called golden rule inversion.

We arrive at the following expression for the pressure as a function of the density ($\alpha^0=\beta\mu^0$):

$$\begin{aligned} p(\{\alpha_c^0\}) &= \sum_a \frac{\zeta_a}{\beta} I_{3/2}(\alpha_a^0) + \sum_a \zeta_a \xi_a \mathcal{I}_{HF}(\alpha_a^0) + p^{MW}(\{\alpha_c^0\}) \\ &\quad + \sum_a p_a^{e^4 n}(\alpha_a^0) - \sum_a \zeta_a \xi_a I_{-1/2}(\alpha_a^0) I_{1/2}(\alpha_a^0) \\ &\quad - \sum_a \frac{I_{1/2}(\alpha_a^0)}{\beta I_{-1/2}(\alpha_a^0)} \frac{\partial}{\partial \alpha_a}[\beta p^{MW}(\{\alpha_c\}) \\ &\quad + \beta p_a^{e^4 n}(\alpha_a)]|_{\alpha_a^0}. \end{aligned} \tag{12}$$

The density can now easily be calculated from $n_a=\zeta_a I_{1/2}(\alpha_a^0)$. For a given density, the chemical potentials for the species are different. Now it is possible to derive expressions for any thermodynamic function. With $U=F-T(dF/dT)$, we get

$$\begin{aligned} \frac{U}{\Omega} &= \frac{3}{2} k_B T \sum_a \zeta_a I_{3/2}(\alpha_a^0) + \sum_a \zeta_a \xi_a \mathcal{I}_{HF}(\alpha_a^0) - p^{MW}(\{\alpha_c^0\}) \\ &\quad - \sum_a p_a^{e^4 n}(\alpha_a^0) - \frac{3}{2} \sum_a \zeta_a \xi_a I_{-1/2}(\alpha_a^0) I_{1/2}(\alpha_a^0) \\ &\quad + T \frac{\partial}{\partial T}\left(p^{MW}(\{\alpha_c^0\},T) + \sum_a p_a^{e^4 n}(\alpha_a^0) \right)\Bigg|_{n=\text{const}}. \end{aligned} \tag{13}$$

These expansions are valid for weakly coupled multicomponent plasmas at any degeneracy. In the $T=0$ limit they reduce to the r_s expansion (r_s is the Brueckner parameter) of Gell-Mann and others [13,16]. In the low density high temperature limit, Eqs. (12) and (13) reduce to density expansions up to $(ne^2)^2$ [17].

In Fig. 4, the results from different types of inversions are compared to each other. It is clearly visible that, especially in the region where no limiting law is valid, one has to be careful in using one approximation or another. Unphysical behavior of the pressure arises if not all terms of a particular order are taken into account. As pointed out before, we prefer the consistent approximation up to order e^4 obtained by the golden rule scheme. The anomalous e^4 exchange term is of higher order at low densities and is compensated at $T=0$ and will thus be omitted from our further discussion. In contrast, the inclusion of the normal e^4 term is necessary for a consistent approximation. The difference between our new e^4

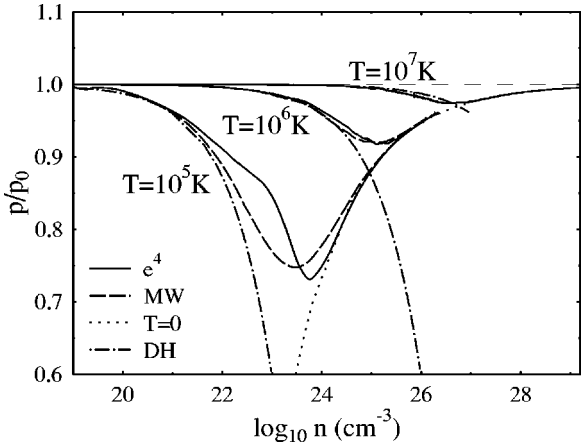

FIG. 5. Pressure of an electron gas normalized by the ideal pressure at different temperatures as function of the density. DH means the nondegenerate Debye–Hückel correction to the ideal gas result. The $T=0$ result is due to Gell-Mann and Brueckner [16]. The dashed curves are in MW approximation; the solid curves take into account also the normal e^4 term [Eq. (12)].

approximation and our older MW scheme (without the normal e^4 term) is essential and can be seen in Fig. 4 (solid line versus long dashed line).

IV. RESULTS AND DISCUSSION

A. The quantum electron gas

Now we want to discuss our results for the EOS and compare our findings with results from different methods. Let us start with the equation of state for an electron gas. Three isotherms for the pressure according to Eq. (12) using the golden rule scheme are shown in Fig. 5. For low and high densities the pressure approaches the ideal result. In these limiting cases it is not necessary to evaluate the full expressions of Eq. (12). As is shown, simple analytical expressions [16,17] describe the pressure with high accuracy. Only in the intermediate range of densities from 10^{21} to 10^{24} cm^{-3} do we find deviations from the limiting slopes. From higher to lower temperatures the minima become more developed and move to lower densities. This is due to the relevance of the interaction terms with respect to the ideal parts of the pressure. At higher densities quantum corrections are of importance and the curves merge into the ideal behavior ($p/p_0=1$). Moreover, it can be seen that the normal e^4 exchange term gives relevant contributions only for lower temperatures. The region of validity of our perturbation expansion has to be proven carefully. We mention that this intermediate region is, at present, not covered by a consequent theory and should, thus, be subject to numerical simulations which could support Padé approximations.

Let us consider additionally the radial distribution function (RDF) which is of interest for many investigations. It is obtained by a functional derivative of the mean potential energy with respect to the interaction potential. From the mean potential energy given by Eq. (6), one may deduce the corresponding approximation for the RDF. Neglecting the

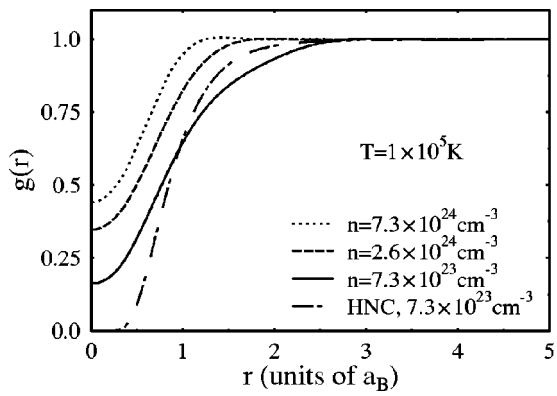

FIG. 6. Radial distribution function for an electron gas at temperature $T=1\times10^5$ K for different densities. Curves not especially denoted are calculated in the e^4 approximation [Eq. (14)].

anomalous e^4 term, the RDF for an electron gas can then be written as

$$g(r)=1+g^{HF}(r)+g^{MW}(r)+g^{e^4n}(r). \tag{14}$$

Using momentum representation the Montroll-Ward and the normal e^4 exchange terms are given by

$$g^{MW}(p)=\frac{2}{n^2}\int\frac{d\omega}{2\pi}\frac{n_B(\omega)}{V_{ee}(p)}[\mathrm{Im}\,\varepsilon^{-1}(p,\omega)-\mathrm{Im}\,\varepsilon(p,\omega)],$$

$$\begin{aligned}g^{e^4n}(p)=-\frac{2m}{n^2}\int\frac{d\mathbf{q}_1d\mathbf{q}_2}{(2\pi)^6}&\frac{V_{ee}(\mathbf{p}+\mathbf{q}_1+\mathbf{q}_2)}{q_1^2+q_2^2-(\mathbf{p}+\mathbf{q}_1)^2-(\mathbf{p}+\mathbf{q}_2)^2}\\&\times\{f(q_1)f(q_2)[1-f(\mathbf{q}_1+\mathbf{p})][1-f(\mathbf{q}_2+\mathbf{p})]\\&-f(\mathbf{q}_1+\mathbf{p})f(\mathbf{q}_2+\mathbf{p})[1-f(q_1)][1-f(q_2)]\}.\end{aligned} \tag{15}$$

After Fourier transformation, the RDF in position space is found. In Fig. 6 results for the RDF of an electron gas are shown. For comparison a RDF calculated by a hypernetted chain (HNC) scheme was drawn. We used a pure Coulomb potential and the ALLNAT algorithm to calculate the HNC RDF. To this density and temperature correspond the following values of the coupling parameter and the degeneracy parameter: $\Gamma=2.4$, $n\Lambda_e^3=9.6$. Whereas the HNC scheme sums up nearly all the interaction contributions but does not account for quantum effects, the opposite is the case for the e^4 approximation of the RDF given by Eqs. (14) and (15). It accounts for correlation and quantum effects up to the order e^4 in a consistent manner. As can be seen in Fig. 6, quantum effects shift the RDF at small distances r to values greater than zero. This is a result of the uncertainty principle, which can also be observed if an effective potential (accounting for quantum effects in lowest order, e.g., a Kelbg potential) is used in the HNC scheme.

B. Fully ionized hydrogen

We find the same qualitative behavior as for the EOS of the electron gas for fully ionized hydrogen, which we want

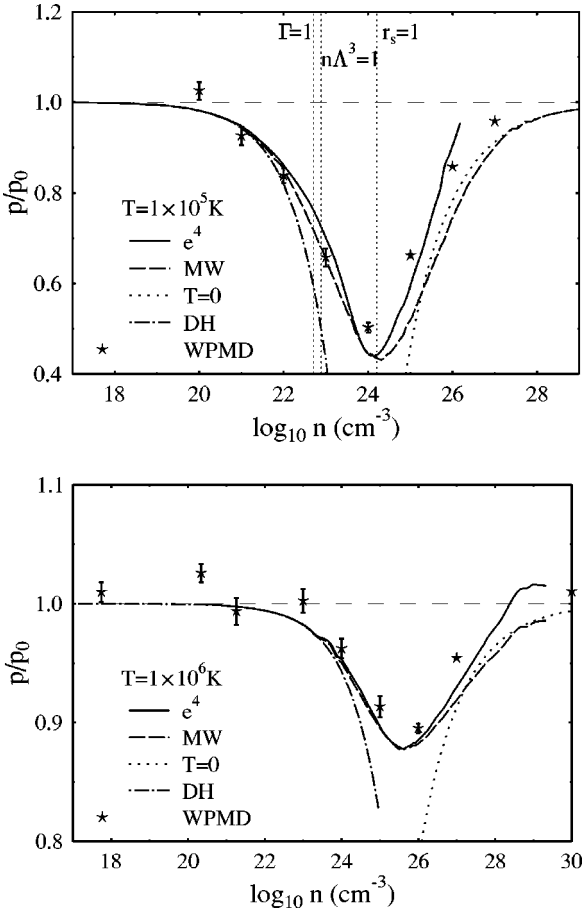

FIG. 7. Pressure of a fully ionized hydrogen plasma normalized by the ideal gas result at $T=10^5$ K (upper) and $T=10^6$ K (lower) as a function of the electron density in different approximations. The WPMD data points were computed by Knaup [20]. The solid line is our e^4 approximation [Eq. (12)], the dashed curve gives the MW approximation. The low density Debye-Hückel result is dash-dotted, whereas the $T=0$ result is dotted. Additionally, some parameters are shown: the classical coupling parameter $\Gamma=e^2/(k_B T d)$ $(d=[3/(4\pi n)]^{1/3}$—mean particle distance), the degeneracy parameter $n\Lambda^3$ (for electrons), and r_s, the nonideality parameter in the quantum case.

to study next. Although hydrogen is the simplest element it shows features which are not easily described, even in thermodynamic equilibrium. Several very different theoretical and numerical methods were developed in the past to overcome those difficulties. We mention here wave-packet molecular-dynamics calculations [18,19] and path integral Monte Carlo simulations [21,22].

In Fig. 7 we show a comparison between different approximation levels of our theory and WPMD results given by Knaup [20] for two different temperatures. The WPMD simulations treat protons as classical particles having both position and momentum and describe the electrons by antisymmetrized wave packets [19]. We find agreement with simulation data especially in the region $n\Lambda_e^3 \leqslant 1$, i.e., for weakly degenerate plasmas. In this region, some of the WPMD data show pressure above $p/p_0=1$, in contrast to our findings. For densities higher than $r_s=1$ deviations begin to grow. Both the MW and e^4 expansions fail to meet the WPMD points. Taking into account the e^4 exchange term leads to a pressure larger than the ideal part. In this region the electrons form a weakly coupled quantum gas and the protons form a strongly coupled classical fluid. Our approach fails to describe these strong correlations. We want to remark that for protons the degeneracy parameter $n\Lambda_p^3$ is equal to unity at $n\approx 6\times 10^{27}$ cm^{-3} for $T=10^5$ K and at $n\approx 2\times 10^{29}$ cm^{-3} for $T=10^6$ K.

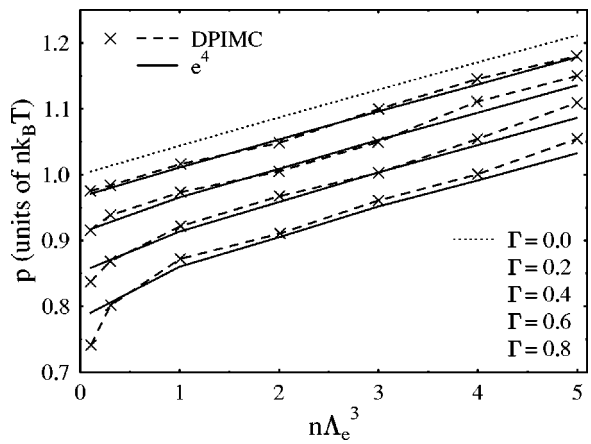

FIG. 8. Pressure of hydrogen as a function of the electron degeneracy parameter $n\Lambda^3$ for different values of the classical coupling parameter $\Gamma=e^2/(k_B T d)$ $(d=[3/(4\pi n)]^{1/3}$—mean particle distance) in different techniques: DPIMC results of Filinov *et al.* [22] (crosses), our results (solid). The value of Γ belonging to a certain curve changes from top to bottom as indicated.

Another numerical method is the PIMC simulation. There are two different techniques called RPIMC (restricted PIMC; Militzer and Ceperley [21]) and DPIMC (direct PIMC; Filinov *et al.* [22]). Both methods use a path-integral representation of the partition function, but they differ in details of the handling of the density matrix and in the solution of the fermion sign problem. Filinov *et al.* use an analytical high temperature expression for the two-particle density matrix, whereas Militzer and Ceperley solve the Bloch equation numerically for the same purpose.

We compare our results to results of both PIMC techniques. First, we show, in Fig. 8, data given by Filinov *et al.* [22] for $\Gamma<1$. There is a very good agreement with less than 0.5% deviation at $\Gamma=0.2$ up to 5% deviation at $\Gamma=0.8$.

A similar good agreement can be found at lower densities in Fig. 9, where we show our results for an isotherm at $T=125\,000$ K together with RPIMC results by Militzer and Ceperley [21]. Additionally we show, in Fig. 9, a low density expansion up to order $(ne^2)^{5/2}$ [17]. For higher densities, as can also be seen in Fig. 10, the simulation data and our results fail to match. This is due to strong correlations, i.e., bound states (hydrogen atoms) and other complexes which change the behavior of the thermodynamic quantities in this parameter region. Additionally, in Fig. 10, the Padé formula results and WPMD data taken from [18] are shown.

V. CONCLUSION

We calculated the equation of state of dense hydrogen in the e^4 approximation using thermodynamic Green's func-

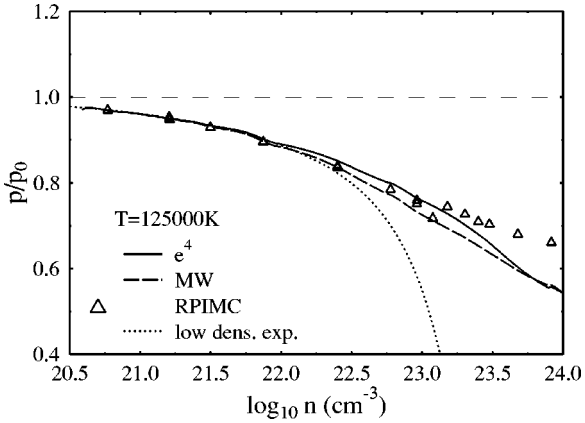

FIG. 9. Pressure of hydrogen with respect to the ideal gas as function of the electron density in different techniques. RPIMC data (triangles) is of Militzer and Ceperley [21], the solid line and the dashed curve are our e^4 [Eq. (12)] and MW approximations, respectively. The short dotted line gives a low density expansion up to $(ne^2)^{5/2}$ due to Riemann *et al.* [17].

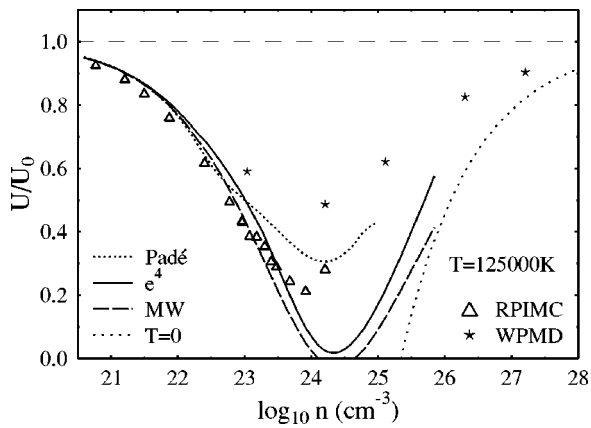

FIG. 10. Internal energy of hydrogen with respect to the ideal gas as a function of the electron density in different techniques. DPIMC data of Militzer [21]; WPMD data of Knaup *et al.* [18]; Padé formula from [23]; the solid and dashed curves are our results. Additionally the $T=0$ limiting result is shown (long dotted).

tions. Our approximation is valid for weakly coupled systems of any degeneracy. In these parameter regions our expansion is of high accuracy. We mention that the inclusion of the exchange contribution of order e^4 gives an essential contribution to the thermodynamic functions for the electrons. From Figs. 4, 6, 7, and 10, one can see that there is some need for further efforts in the intermediate density region, which should be covered by numerical experiments.

We compared our results to those of very different simulation methods. For $\Gamma<1$ we found good agreement with all of those techniques. Some of the WPMD results showed larger deviations from our results than the PIMC data. For higher coupling we must state that our approach is not good enough to describe the strong coupling in the proton subsystem. Strong coupling may also occur in systems of ions in a trap [24]. In ion systems and in the proton subsystem the exchange contribution ne^4 does not give an essential contribution. However, the approximation up to the MW term is sufficient only for small Γ values; for higher ones one should add (classical) HNC based contributions to the pressure. The physical situation becomes easier to describe again when the ideal part of the pressure of the degenerate electron gas dominates, and additionally the protons become degenerate. For this situation up to now there exist no simulation data for comparison. A future task will be the inclusion of higher order correlations, which will allow the approach presented here to be applied to strongly coupled degenerate quantum plasmas. Furthermore, it would be of interest to consider the region where protons behave like Fermi particles and compare our results to simulations.

ACKNOWLEDGMENTS

We gratefully acknowledge collaboration and discussions with Burkhard Militzer, Michael Knaup, and Vladimir Filinov. We want to thank B. Militzer, V. Filinov, and M. Knaup for providing simulation data. This work was supported by the Deutsche Forschungsgemeinschaft through SFB 198 ‘‘Kinetik partiell ionisierter Plasmen.’’

[1] L.B. Da Silva *et al.*, Phys. Rev. Lett. **78**, 483 (1997).
[2] M.D. Knudson *et al.*, Phys. Rev. Lett. **87**, 225501 (2001); **90**, 035505 (2003); J. Phys. A **36**, 6149 (2003).
[3] W.J. Nellis, Phys. Rev. Lett. **89**, 165502 (2002).
[4] B. Militzer *et al.*, Phys. Rev. Lett. **87**, 275502 (2001).
[5] M. Knaup, P.G. Reinhard, C. Toepffer, and G. Zwicknagel, J. Phys. A **36**, 6165 (2003).
[6] H. Juranek, V. Schwarz, and R. Redmer, J. Phys. A **36**, 6181 (2003).
[7] W. Stolzmann and T. Blöcker, Astron. Astrophys. **361**, 1152 (2000).
[8] L.P. Kadanoff and G. Baym, *Quantum Statistical Mechanics* (Addison-Wesley, Redwood City, CA, 1962).
[9] W. Ebeling, W.D. Kraeft, and D. Kremp, *Theory of Bound States and Ionization Equilibrium in Plasmas and Solids* (Akademie-Verlag, Berlin, 1976).
[10] W.D. Kraeft, D. Kremp, W. Ebeling, and G. Röpke, *Quantum Statistics of Charged Particle Systems* (Akademie-Verlag Berlin, 1986).
[11] W.D. Kraeft *et al.*, Z. Phys. Chem. (Munich) **204**, 199 (1998).
[12] H.E. DeWitt, J. Nucl. Energy, Part C **2**, 27 (1961).
[13] L. Onsager, L. Mittag, and M.J. Stephen, Ann. Phys. (N.Y.) **18**, 71 (1966).
[14] W. Stolzmann and W.D. Kraeft, Ann. Phys. (Leipzig) **36**, 387 (1979).
[15] A. L. Fetter and J. D. Walecka, *Quantum Theory of Many-Particle Systems* (McGraw-Hill, New York, 1971).
[16] M. Gell-Mann and K.A. Brueckner, Phys. Rev. **106**, 364 (1957).
[17] J. Riemann, M. Schlanges, H.E. DeWitt, and W.D. Kraeft, Physica A **219**, 423 (1995); J. Riemann, M. Schlanges, and W.D. Kraeft, Laser Part. Beams **15**, 533 (1997).

[18] M. Knaup, P.-G. Reinhard, and C. Toepffer, Contrib. Plasma Phys. **41**, 159 (2001).
[19] M. Knaup, P.-G. Reinhard, C. Toepffer, and G. Zwicknagel, Comput. Phys. Commun. **147**, 202 (2002).
[20] M. Knaup (private communication).
[21] B. Militzer, Ph.D. thesis, University of Illinois, Urbana, IL, 2000; B. Militzer and D.M. Ceperley, Phys. Rev. E **63**, 066404 (2001).
[22] V.S. Filinov, M. Bonitz, W. Ebeling, and V.E. Fortov, Plasma Phys. Controlled Fusion **43**, 743 (2001).
[23] P. Haronska, D. Kremp, and M. Schlanges, Wiss. Z. Univ. Rostock, Naturwiss. Reihe **36**, 98 (1987).
[24] D.H.E. Dubin and T.M. O'Neil, Rev. Mod. Phys. **71**, 87 (1999).